Optical and Quantum Electronics **36:** 349–366, 2004.

Minimization of the pulse's timing jitter in a dispersion-compensated WDM system

OFIR AHARON[1,*], BORIS A. MALOMED[2,3], Y.B. BAND[1,4] AND U. MAHLAB[3,5]
[1]*Department of Electro-Optics, Ben Gurion University of the Negev, Beer-Sheva 84105, Israel*
[2]*Department of Interdisciplinary Studies, Faculty of Engineering, Tel Aviv University, Tel Aviv 69978, Israel*
[3]*ECI Telecom Ltd, Optical networks division, 30 Hasivim street, Petach Tikva 49517, Israel*
[4]*Department of Chemistry, Ben Gurion University of the Negev, Beer-Sheva 84105, Israel*
[5]*Department of Electrical Engineering, Holon Academic Institute of Technology (HAIT), Holon 58102, Israel*
*(*author for correspondence: E-mail: oaharon@bgumail.bgu.ac.il)*

Received 1 September 2003; accepted 12 December 2003

Abstract. We address the problem of the collision-induced crosstalk between pulses in a dispersion-compensated WDM system composed of a periodic array of cells that include two or three fiber segments. Both the cross- and self-phase-modulation nonlinearities are taken into account. A semi-analytical approximation and direct simulations are used to calculate the frequency shift (FS) of colliding pulses, and to search for conditions which provide for minima of the FS and the temporal shift (TS), including the most promising possibility of minimizing both shifts simultaneously. Semi-analytical results, obtained by means of the perturbation theory, are in qualitative agreement with the numerical findings, especially in regimes near the optimum. In searching for the FS and TS minima, we investigate the effect of changing the initial width and chirp of the pulse, position of the amplifier within the dispersion–compensation period, group-velocity difference between the channels, allocation of the group-velocity-dispersion (GVD) inside the cell, and the average GVD. We conclude that a more sophisticated dispersion–compensation map, with *three* different local values of GVD, may be significantly more efficient than the one based on two different segments. A global FS minimum, with respect to the variation of all the parameters, is found.

Key words: cross-phase modulation (XPM), dispersion–compensation (DC), frequency shift (FS), time jitter

1. Introduction

It is well known that periodic dispersion compensation is a necessary ingredient of fiber-optic communication networks (Iannone *et al.* 1998). In its simplest realization, dispersion compensation (which, in the case of return-to-zero (RZ) pulses, is frequently called dispersion management, or DM for brevity Berntson *et al.* 1998) is realized as periodic alternation of fiber sections with anomalous and normal group-velocity dispersion (GVD). Dispersion compensation was originally introduced in order to minimize dispersion-induced distortion of quasi-linear (nonsoliton) pulses inside data-

transmission channels (Kurtzke 1993; Ablowitz *et al.* 2001). Later, it was demonstrated that it also helps suppress nonlinear crosstalk between channels in wavelength-division multiplexed (WDM) systems (Sugahara *et al.* 1997; Kaup *et al.* 1998, 1999; Niculae *et al.* 1998; Haus and Chen 1999; Ablowitz *et al.* 2001, 2002; Etrich *et al.* 2001; Sugahara 2001; Sugahara and Maruta 2001; McKinstrie 2002). Crosstalk is induced by interaction of pulses (solitons are often considered in this context) belonging to different channels *via* the cross-phase modulation (XPM) and four-wave mixing. Collisions between pulses, that have different velocities in different channels, give rise to frequency and temporal-position shifts of the pulses. This is the source of additional timing jitter that impedes achievement of higher bit rates in WDM systems.

In the consideration of interactions between pulses belonging to different channels, one should distinguish between *complete* and *incomplete* collisions. In the former case, the pulses are initially widely separated, and the faster pulse overtakes the slower one. In the latter case, the solitons are partially or completely overlapped at the initial point, $z = 0$, where they are launched into the fiber link. Generally, incomplete collisions are more treacherous, as they give rise to larger frequency shift (FS), which will then be translated, *via* GVD, into a time shift (TS) linearly growing with the propagation distance z (Hirooka and Hasegawa 1998; Kaup *et al.* 1998, 1999; Haus and Chen 1999). The statistical contribution of complete collisions is larger in a long-haul system, but, as the collision length for solitons is, typically, ~ 500 km or larger (see, e.g., Kaup *et al.* 1998, 1999), this may not overweigh the crucially important role of the incomplete collisions in moderately long links. Therefore, in this work we focus on the worst case of the incomplete collision, when the centers of the two pulses coincide at the point $z = 0$.

The FS and TS produced by pair-wise collisions between solitons in WDM-DM systems were calculated both analytically (Hirooka and Hasegawa 1998; Kaup *et al.* 1999; Sugahara *et al.* 1999; Malomed 2002) and numerically (Sugahara *et al.* 1997, 1999; Kaup *et al.* 1999; Sugahara 2001; Sugahara and Maruta 2001). In particular, it was found that the variational approximation, which is generally an efficacious technique for analysis of various dynamical effects involving solitons in nonlinear optical fibers (see Malomed 2002 for a review), provides good accuracy in predicting results of both complete and incomplete inter-channel collisions in WDM-DM systems (Kaup *et al.* 1999; Ablowitz *et al.* 2001; Mckinstrie 2002). Analytical and numerical results demonstrate that strong DM (with relatively large local GVD values and small average dispersion) is indeed efficient in suppression of the crosstalk.

While a majority of the above-mentioned work has dealt with solitons, the case of major practical interest for applications to fiber-optic telecommunications is crosstalk between quasi-linear pulses. Another essential feature of

real systems is *lumped* (i.e., discrete, along z) amplification, while most theoretical work assumed local compensation between fiber loss and amplification, so that the models were effectively lossless. In this work, our objective is to select parameters of the system providing for minimization of crosstalk effects generated by XPM interaction between nonsoliton pulses in adjacent channels. Assuming the amplification spacing equal to the DM period, we make use of an obvious parameter available for optimization, viz., the location of amplifiers inside the DM map.

The paper is organized as follows. The model is described in Section 2. Relations between normalized units, used in the model, and their physical counterparts are also given in Section 2. Section 3 gives an account of our semi-analytical approach used to treat the XPM-induced FS. Direct numerical simulations and findings of a search for a regime that minimizes the FS are presented in Section 4. Further results, including a generalization dealing with the dispersion map consisting of three segments, and comparison of numerical and semi-analytical results, are presented in Section 5. Section 6 contains the summary and conclusions.

2. The model

We adopt the standard model of the two-channel DM system, based on coupled nonlinear Schrödinger (NLS) equations for slowly varying amplitudes U and V of the electromagnetic waves in two wavelength-separated channels. The equations are taken in the usual form (see, e.g., Kaup *et al.* 1999):

$$\mathrm{i}(U_z + c(Z)U_\tau) + \frac{1}{2}D(Z)U_{\tau\tau} + \varepsilon\left[\frac{1}{2}\overline{D}_u U_{\tau\tau} + \gamma(Z)(|U|^2 + 2|V|^2)U\right] + \frac{\mathrm{i}}{2}[\alpha - G(Z)]U = 0,$$

$$\mathrm{i}V_z + \frac{1}{2}D(Z)V_{\tau\tau} + \varepsilon\left[\frac{1}{2}\overline{D}_v V_{\tau\tau} + \gamma(Z)(|V|^2 + 2|U|^2)V\right] + \frac{\mathrm{i}}{2}[\alpha - G(Z)]V = 0.$$

Here Z and τ are the propagation distance and reduced time, subscripts stand for the partial derivatives, $D(Z)$ is the effective local GVD coefficient ($D = -2\pi c\beta_2/\lambda^2$, where $\beta_2(Z)$ is the local GVD coefficient proper, and λ is the carrier wavelength) corresponding to the periodic alternation of fiber segments with anomalous ($D > 0$) and normal ($D < 0$) dispersion, while $\overline{D}_u$ and $\overline{D}_v$ are average values of the GVD coefficients in the two channels (which, generally, differ due to third-order dispersion). The nonlinear coefficients

$\gamma(Z)$ are also different in the fibers with the anomalous and normal dispersion; for instance, $\gamma_1 = 1.267\ (\mathrm{W\,km})^{-1}$ in the standard single-mode fiber with the negative dispersion (which is known as the G.652 fiber), while the ordinary dispersion-compensating fiber providing for the positive dispersion has $\gamma_2 = 5.067\ (\mathrm{W\,km})^{-1}$. Finally, the coefficient c in the above equations is the inverse group-velocity difference between the channels, and α is the fiber-loss parameter; both c and α may also be different in the two fiber species.

The above equations can be normalized to make the effective nonlinearity coefficients in both of them constant (z-independent) and equal to unity. Indeed, dividing the equation inside each segment by the respective coefficient $\gamma_{1,2}$, we can locally redefine the propagation distance, so that $\gamma_{1,2}\mathrm{d}Z \equiv \mathrm{d}z$, and the dispersion coefficient, so that $D(Z)$ is replaced by $D(z) \equiv D(Z)/\gamma(Z)$. Note that, taking into regard the above-mentioned typical values of the fiber nonlinearity coefficient, the rescaling of the coordinate Z implies an effective relative stretch of the normal-dispersion segment, roughly speaking, by the factor of 4; this is, however, compensated by the proportional weakening of the rescaled normal dispersion against its anomalous counterpart.

Further, the original loss parameter α is replaced by the rescaled one, $\alpha(z) \equiv \alpha/\gamma(Z)$, and c is replaced by $c(z) \equiv c/\gamma(Z)$. Actually, in the resultant equations it is sufficient to replace the latter two coefficients by their constant values averaged over the dispersion–compensation cell (this will be clear from the subsequent analysis). We note that, as in the case of the GVD coefficient, the strong stretching of the normal-dispersion segment due to the rescaling of the coordinate is essentially compensated by the inverse rescaling of the loss and inverse-group-velocity parameters in that segment, although, in the general case, their average values in the rescaled model are not the same as in the unrescaled one.

Thus, we obtain rescaled equations in the form

$$\mathrm{i}(U_Z + cU_\tau) + \frac{1}{2}D(z)U_{\tau\tau} + \varepsilon\left[\frac{1}{2}\overline{D}_u U_{\tau\tau} + \gamma(z)\left(|U|^2 + 2|V|^2\right)U\right] + \frac{\mathrm{i}}{2}[\alpha - G(z)]U = 0, \tag{1a}$$

$$\mathrm{i}V_Z + \frac{1}{2}D(z)V_{\tau\tau} + \varepsilon\left[\frac{1}{2}\overline{D}_v V_{\tau\tau} + \gamma(z)\left(|V|^2 + 2|U|^2\right)V\right] + \frac{\mathrm{i}}{2}[\alpha - G(z)]V = 0. \tag{1b}$$

Relations between normalized units implied in Equations (1a) and (1b) and their physical counterparts will be given below.

In the above formulation, the average value of $D(z)$ is zero by definition, the average dispersion being represented solely by $\overline{D}_u$ and $\overline{D}_v$. Furthermore, we define

$$N(z) \equiv \left\{ \begin{array}{ll} D_1, & 0 < z < L_1 \\ D_2, & L_1 < z < L_1 + L_2 + d \end{array} \right\}, \tag{1c}$$

$$D(z) = \sum_k N(z - kL_t)[H(z - kL_t) - H(z - (k+1)L_t)], \tag{1d}$$

where $L_t \equiv L_1 + L_2 + d$ is the total DM period (see Fig. 1), and H is the Heaviside step function. The small parameter ε is introduced in Equations (1a) and (1b) to label terms that are to be treated as perturbations in the strong-DM regime (see Kaup *et al.* 1999).

To compensate the loss accounted for by the coefficient α, Equations (1a) and (1b) include the lumped amplification (gain), which is given by

$$G(z) = G_0 \sum_k \delta(z - L_t k - d), \tag{2}$$

where G_0 is the gain of an individual amplifier, d is the position of the amplifier relative to the DC map (see Equations (1c), (1d) and Fig. 1). Pursuant to what was said above, the amplification spacing is set equal to the DM period L_t.

As mentioned above, the amplifier's position parameter d may be employed to minimize the collision-induced FS. Fig. 1 and Equations (1c) and (1d) imply that the length of the anomalous-dispersion segment (the one with $D(z) > 0$) is L_1, while the normal-dispersion segment (the one with $D(z) < 0$),

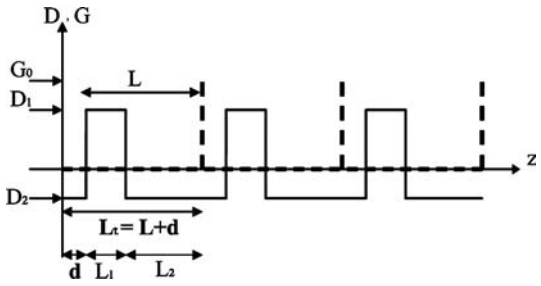

Fig. 1. The simplest scheme of the dispersion compensation (one channel is shown). Solid and dashed lines represent, respectively, the distribution of the local dispersion and gain. The average dispersion is excluded from the profile of $D(z)$ shown in this figure, see Equation (1).

whose total length is $L_2 + d$, is split into two parts, to distinguish the parameter d.

Following Liu *et al.* 2003, we adopt the following normalizations for the lengths of the anomalous- and normal-dispersion segments in the DM map shown in Fig. 1 and the corresponding values of the local dispersions (which can always be achieved by means of obvious rescalings):

$$L_1 D_1 = (L_2 + d)|D_2| \equiv 1, \quad L_1 + L_2 + d \equiv 1. \tag{3}$$

In particular, the first condition in this set guarantees that the proper average dispersion of the map (1c), (1d) is indeed zero, so that only the coefficients $\overline{D}_u$ and $\overline{D}_v$ are responsible for the average GVD in Equations (1a) and (1b).

In addition to the simplest scheme displayed in Fig. 1, in Section 5 we also consider a more sophisticated one, shown in Fig. 2, in which the segment of the length d, between the amplifier and the junction of the anomalous-dispersion and normal-dispersion fibers, is given its own local GVD coefficient, D_3, that can be different from D_2 (in this case, the first normalization condition in Equation (3) is replaced by Equation (7), see below). It will be demonstrated that using this extra parameter in the minimization of the collision-induced FS turns out to be quite beneficial.

For the interpretation of results displayed below, it is necessary to establish relations between normalized variables and parameters used in Equations (1)–(3) and the corresponding quantities in physical units. To this end, we notice that if $\tau = 1$ corresponds to t_0 picoseconds in physical units (a typical value of the temporal width of pulses used in fiber-optic networks, that may be taken as 20 ps, to safely provide for the per-channel bit-rate of 10 Gb/s), and the physical value of the dispersion coefficient is D_0 ps^2/km (most typically, it is 20 ps^2/km for the standard telecommunications fiber, and 2 ps^2/km

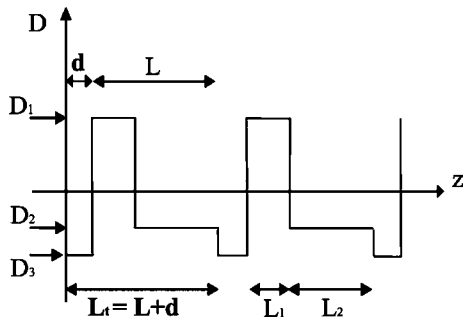

Fig. 2. The DM map with three different local values of the GVD coefficient. Investigating this scheme, we fixed the values $L_1 = 2/5$, $D_1 = 5/2$, $L_2 = 3/5$, $D_2 = -5/3$, while D_3 and d were varied.

for the dispersion-shifted one), then $z = 1$ corresponds to the propagation distance $D_0 t_0^2$ in kilometers. In fact, we will typically be dealing with normalized pulse widths in a ballpark of $\tau_0 \sim 1$, that indeed suggests to set $t_0 = 20\,\text{ps}$, which is assumed below. The amplification spacing (equal to the total GVD-compensation period), which is normalized to unity in the present model, is, typically $\approx 80\,\text{km}$ in physical units, suggesting the choice of $D_0 = 0.2\,\text{ps}^2/\text{km}$. Then, the remaining normalization conditions in Equation (3) imply (for the case of the dispersion-shifted fiber) a typical local value of the GVD coefficient $D \sim 5$, in the normalized units.

The physical value of the inverse-group-velocity difference between channels is $c_{\text{phys}} = (t_0/z_0)c$, where c is the normalized average inverse-group-velocity difference in Equation (1a). On the other hand, the same parameter can be expressed in terms of the wavelength difference $\Delta\lambda$ between the channels according to the definition of the average GVD coefficient $\overline{D}$:

$$c_{\text{phys}} = \frac{2\pi s_0 \overline{D}}{n\lambda^2}\Delta\lambda.$$

Here s_0 is the light velocity in vacuum, n is the refractive index, and λ is the carrier wavelength. In the results displayed below, the normalized inverse-group-velocity difference ranges around $c \sim 1$, which corresponds to $c_{\text{phys}} \sim 0.25\,\text{ps/km}$, with regard to the above-mentioned characteristic units, $t_0 = 20\,\text{ps}$ and $z_0 = 80\,\text{km}$ (for the estimate, we adopt $n = 1.5$, and $\lambda = 1.5\,\mu\text{m}$). On the other hand, taking the average GVD coefficient $\overline{D} \sim 1\,\text{ps}^2/\text{km}$, the above expression for c_{phys} in terms of $\Delta\lambda$ shows that $c_{\text{phys}} \sim 0.25\,\text{ps/km}$ corresponds to the wavelength difference between the channels $\Delta\lambda \sim 0.5\,\text{nm}$, which is a typical value of interest for the modern-day WDM systems.

The physical loss and gain parameters, measured respectively in dB/km and dB, are expressed in terms of their normalized counterparts in Equation (1) as follows: $\alpha_{\text{phys}} = (10/\ln 10)\alpha/z_0$, and $G_{\text{phys}} = (10/\ln 10)G$ (recall that α is actually the normalized loss parameter averaged over the dispersion–compensation cell).

The values given above can be used to translate results displayed below in the dimensionless form into physical units. However, as concerns the parameters d and D_3, which, together with the average GVD coefficients $\overline{D}_u$ and $\overline{D}_v$ are the essential ones employed for the minimization of the collision-induced effects, most relevant results for their optimum values are expressed in the dimensionless form, as this makes it easy to compare, respectively, the optimum value of d with the amplification spacing (alias dispersion–compensation period), and the values of $\overline{D}_u$, $\overline{D}_v$ and D_3 with the local GVD coefficients. Lastly, the initial *chirp* C of pulses in Equations (4a) and (4b), see below, is defined in such a way that it is always dimensionless.

3. The semi-analytical method

Semi-analytical studies of crosstalk effects were performed previously (Kaup *et al.* 1999) without taking into account the loss and periodic amplification. In this section, we develop an approach that explicitly incorporates those factors. This is an important issue, as crosstalk effects are nonlinear in their character, hence they may be essentially affected by the periodic variation of the pulse's amplitude under to the combined action of the loss and gain.

It is assumed that Gaussian pulses, which represent nonsoliton (quasi-linear) signals, are launched in the two channels at the point $z = 0$, with equal peak powers A_0^2, temporal width τ_0 and relative (dimensionless) chirp C:

$$U_0 = A_0 \exp\left(-(1 + \mathrm{i}C)\frac{(\tau - T_0)^2}{\tau_0^2}\right), \tag{4a}$$

$$V_0 = A_0 \exp\left(-(1 + \mathrm{i}C)\frac{\tau^2}{\tau_0^2}\right). \tag{4b}$$

Here T_0 is the initial temporal separation (delay) between the two pulses. As indicated above, we consider only the case $T_0 = 0$, i.e., the pulses completely overlapping at $z = 0$, since this case is known to be the most problematic one, giving rise to the largest FS.

In the linear limit (dropping the XPM and SPM (self-phase modulation) terms), Equations (1a) and (1b) are decoupled, and have well-known exact solutions in the form of Gaussians. In the U-channel, the solution is

$$U(z,\tau) = \frac{\sqrt{P_0}a_0}{\sqrt{a_0^2 + 2\mathrm{i}\Delta(z)}}\exp\left(-\frac{1}{2}\alpha z + \frac{1}{2}\int_0^z G(z)\,\mathrm{d}z\right)\exp\left(-\frac{\tau^2}{a_0^2 + 2\mathrm{i}\Delta(z)}\right), \tag{4c}$$

where the accumulated dispersion is defined as

$$\Delta(z) \equiv \Delta_0 + \int_0^z D(z)\,\mathrm{d}z, \tag{5a}$$

and a_0 is the smallest pulse width, attained at the point where $\Delta(z) = 0$. The constants a_0, Δ_0 and P_0 may be used as a natural set of parameters characterizing the Gaussian pulse – in lieu of τ_0, C and A_0^2 – as proposed in Kaup *et al.* (1999). Relations between the two sets can be readily obtained from the comparison of Equations (4a) and (4c):

$$\tau_0 = a_0^{-1}\sqrt{a_0^4 + 4\Delta_0^2}, \quad C = 2\Delta_0 a_0^{-2}, \tag{5b}$$

$$A_0^2 = \frac{P_0 a_0^2}{\sqrt{a_0^4 + 4\Delta_0^2}}. \tag{5c}$$

In terms of physical quantities, the parameter Δ_0, used below for the optimization (although it will be found that it produces little effect, unlike other parameters), can be expressed, pursuant to Equations (4) and (5b), as follows: $\Delta_0 = (C/2)[(a_0)_{\text{phys}}/t_0]^2$, where $(a_0)_{\text{phys}}$ is the smallest temporal width of the pulse, measured in ps, and C is the relative (dimensionless) chirp defined as in Equation (4).

The central-frequency shift of the wave V is defined as follows:

$$\delta\omega \equiv \left| \frac{\int_{-\infty}^{\infty} \omega \cdot |V(z,\omega)|^2 \, \mathrm{d}\omega}{\int_{-\infty}^{\infty} |V(z,\omega)|^2 \, \mathrm{d}\omega} \right|. \tag{5d}$$

This definition is used below to calculate FS in numerical simulations as well.

Semi-analytical results for the FS can be obtained by direct application of a general formula derived in Kaup *et al.* (1999) by means of the perturbation theory, treating each pulse as a quasi-particle, with a force of interaction between them induced by XPM. Taking into account the additional evolution of the pulses under the action of the loss, and skipping details of the algebra (which are similar to those elaborated in Kaup *et al.* 1999), we arrive at the following integral expression for the collision-induced FS, derived from the above-mentioned formula borrowed from Kaup *et al.* (1999):

$$\delta\omega = \int_0^{Z_{\max}} \frac{2^{3/2}\varepsilon P(z) T_0^4 c \cdot z}{[T_0^4 + 4\Delta^2(z)]} \cdot \exp\left(-\frac{(cT_0 \cdot z)^2}{[T_0^4 + 4\Delta^2(z)]} \right) \mathrm{d}z, \tag{5e}$$

where we have defined

$$P(z) \equiv \sum_k G_0 \exp\left(-\frac{\alpha}{2}[z - (k-1)L_t] \right) [H(z - (k-1)L_t) - H(z - kL_t)]. \tag{5f}$$

The integrals in these expressions will be computed numerically, and the ensuing results will be compared below with those obtained from direct simulations of the underlying Equation (1).

Table 1. Pairs of normalized parameters varied for the optimization (a relation between the normalized and physical units is described in the text)

Case 1	
τ_0	0.5:0.02:2
d	0:0.02:1
Case 2	
Δ_0	−3:0.1:3
τ_0	0.5:0.02:2
Case 3	
Δ_0	−3:0.1:3
d	0:0.02:1
Case 4	
D_3	−8:0.1:5
D	0:0.02:1
Parameter	Meaning
τ_0	Initial width of the pulse
d	Location of the amplifier in the DM cell
Δ_0	Initial chirp of the pulse
D_3	Altered dispersion value in the section of length d

The notation $P_{\min} : \Delta P : P_{\max}$ implies that the parameter P was varied between the limits $P_{\min}$ and $P_{\max}$ with the step of ΔP. The physical meaning of the parameters is explained in the table too.

4. Direct simulations

4.1. PARAMETER REGIMES

Simulations of the evolution of two identical Gaussian pulses whose centers coincide at the initial point, $z = 0$, were run for four sets of normalized parameters given in Table 1. The pulses were propagated over 10 DM periods. The gain G_0 in Equation (2) was adjusted to other parameters so that to maintain a constant value of the pulse's peak power in the simulations (which remains equal to the initial value).

Numerically determined values of the FS ($\delta\omega$) and TS (δT) were collected after passing each DM period, for all the cases indicated in Table 1. For example, Fig. 3 displays values of FS, for $\overline{D}_{u,v} = -1$, found after the pulse has passed three DM periods (longer propagation does not alter the results in this case; values of other parameters pertaining to Fig. 3 are given in Table 2). The first conclusion following from this figure is that a range where FS takes very small values can be easily identified.

Results of systematic numerical simulations are collected in Figs. 4 and 5, which show the FS and TS versus different pairs of control parameters. In many cases, regions where the shifts are small are evident (see discussion below).

Using the accumulated data, we carried out an optimization procedure with respect to the variation of the parameters d, D_3, Δ_0, $\overline{D}_{u,v}$, c, and τ_0. Other

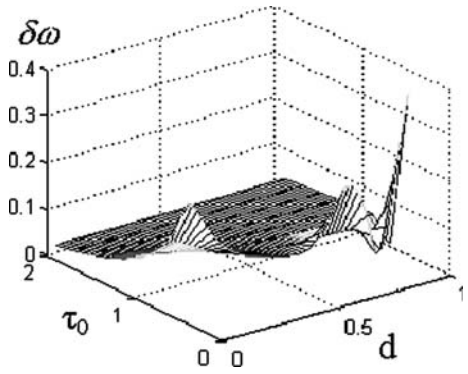

Fig. 3. The collision-induced FS versus the pulse width τ_0 and length d, for $\overline{D}_{u,v} = -1$, after the propagation through three DM periods.

Table 2. Values of other parameters used in simulations

Parameter	Meaning	Value
c	Inverse-group-velocity difference between the channels (see Kaup *et al.* 1999)	0.4
$D(z)$	Local dispersion coefficient, defined as $D = -2\pi c\beta_2/\lambda^2$, where β_2 is the GVD	See Equation (1d)
α	Loss coefficient	ln(10)
G_0	Gain compensating the loss	adjusted in the course of simulations.
$\overline{D}_u$, $\overline{D}_v$	Average values of the dispersion in the two channels	−1
L_1	Length of the anomalous-dispersion segment (with $D > 0$)	0.4
L_2	Length of the normal-dispersion segment (with $D < 0$)	0.6
L	Period of DM without adding the section d	$L_1 + L_2$
L_t	Full DM period	$L + d$
z_k	Amplification spacing	$= L_t$
ε	Formal perturbation parameter in the quasi-linear strong-dispersion-management regime	0.1
$D_{1,2,3}$	Dispersion coefficients in the two-step DM map (for values of D_3 in the three-step DM map, see Figs. 5 and 6)	5/2, −5/3, −5/3
A_0^2	Peak power of the pulse	1 mW

parameters (in particular, the peak power of the pulse and the amplification spacing) were held constant at values indicated in Table 2 (either no significant change of the FS was obtained upon varying those parameters within reasonable limits in both the two- and three-step setups, or their variation is not relevant as they are fixed by material characteristics of the fibers).

In most cases, we chose nonsymmetric DM. For example, we took $L_1 = 2/5$, $L_2 + d = 3/5$, then, according to Equation (3), we had to set $D_1 = 5/2$, $D_2 = -5/3$. As concerns the loss parameter, we took into account

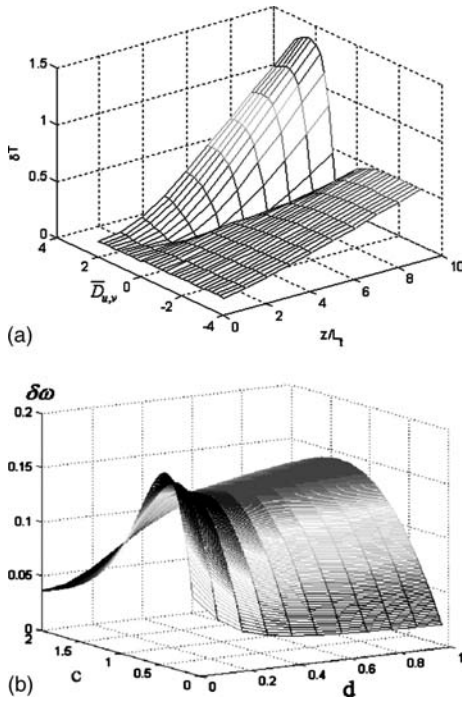

Fig. 4. (a) The collision-induced TS δT versus the normalized propagation distance z/L_t and average dispersion $\overline{D}_{u,v}$, for $d = 0.4$, $\tau_0 = 1$, $\Delta_0 = -0.8$, $D_3 = D_2 = -5/3$, and $c = 0.4$. (b) The FS versus c and d after the passage of seven dispersion–compensation periods.

that the peak power of the pulse passing an amplifier spacing is typically attenuated by a factor of 10, hence, in the present notation (with $L = 1$, which coincides with the amplification spacing), we set $\alpha = \ln(10)$. These parameter values can be easily translated into physical ones as described above.

4.2. DEPENDENCE ON THE AVERAGE DISPERSION ($\overline{D}_{u,v}$)

It is well known that the average GVD is an important parameter that strongly affects the pulse transmission in DM systems. To check the influence of the average dispersion on the TS, which expresses the eventual effect of the collision, we ran the simulations taking common values of the average GVD in the two channels as $\overline{D}_{u,v} = -3{:}0.1{:}3$ (i.e., varying them between -3 and $+3$ with a stepsize of 0.1), while other parameters were held constant, $d = 0.4$, $\tau_0 = 1$, $\Delta_0 = -0.8$, $D_1 = 5/2$, $D_3 = D_2 = -5/3$, and $c = 0.4$. However, the propagation length was varied too, as one may naturally expect that, once the collision gives rise to a FS, the resultant TS will grow with distance. The

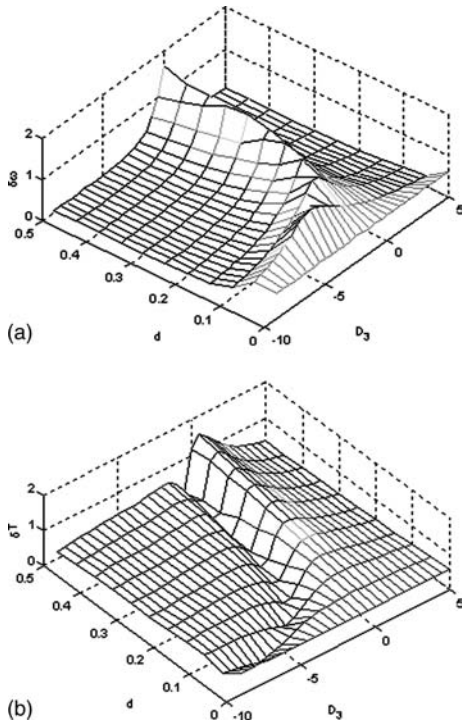

Fig. 5. The FS (a) and TS (b) after the passage of 10 periods, for the case of $L_1 = 0.2$, $L_2 = 0.8$, $c = 0.4$, $D_1 = 3$, $D_2 = -0.75$, in the three-step model with $D_3 \neq D_2$.

results are shown in Fig. 4(a). The pulse is stable in the whole region of small values of $\overline{D}_{u,v}$, but, at the edges of the interval considered, the temporal width of the pulse starts to grow abruptly.

As is seen from Fig. 4(a), the TS indeed strongly depends on the average dispersion. The minimum of the TS in Fig. 4(a) is found around $\overline{D}_{u,v} = 0$. Variation of the parameters d, τ_0, Δ_0, and D_3 leads to moderate changes of the size of the minimum and its location (in terms of the value of $\overline{D}_{u,v}$). It should be noted that, for some parameter values, while the collision-induced shifts remain small, the pulses may suffer considerable distortion at large values of the propagation distance (eight DM periods or more). These parameters are considered as unacceptable for the operation of the system.

4.3. DEPENDENCE ON CHANNEL SEPARATION AND AMPLIFIER LOCATION

Next, we examined how the collision-induced FS are affected by the inverse-group-velocity difference c, which determines the channel density in the

WDM system, and, simultaneously, by the amplifier's position d. In this case, we fixed the initial pulse width τ_0 and chirp Δ_0. The results, obtained after having passed seven DM periods (to make it sure that the pulses have completely separated), are displayed in Fig. 4(b).

Increasing c, we expect a decrease of the FS, since, for small c, the two pulses remain overlapped longer, which should result in a bigger FS. However, Fig. 4(b) (which does not include very small values of c, as the interaction between the pulses is indeed very strong in this case and makes the results unusable) shows that this is not always true. Detailed consideration of the numerical results demonstrates that the dependence of the FS on c is strongly affected by asymmetric deformations of the pulses caused by the collision. The deformations make the resulting FS larger.

5. Further analysis: The three-segment model, and comparison with the semi-analytical predictions

Further inspection of numerical data suggests that a relevant range of the pulse-width parameter τ_0, in which an optimum regime (providing for minimum of the FS) should be sought for, is $0.5 < \tau_0 < 2$. Outside this interval, the pulse quickly spreads out and loses its shape, if $\tau_0 < 0.5$, or the FS simply does not vary much, if $\tau_0 > 2$ (therefore, it makes sense to focus on shorter pulses that provide for a higher bit rate). Another conclusion suggested by the numerical data is that, in order to minimize the FS, d should be taken from the interval (0.1,0.3). Unlike τ_0 and d, the initial chirp Δ_0 does not seem to have an appreciable effect on the FS.

5.1. MINIMIZING FS BY MEANS OF THE THREE-SEGMENT DM MAP

So far, we only considered the dispersion–compensation scheme with two segments L_1 and $L_2 + d$, whose GVD coefficients are D_1 and D_2 (Fig. 1). Further simulations demonstrate that independently adjusting the value of the GVD coefficient, D_3, in the segment of length d makes it possible to suppress the asymmetric distortion of the interacting pulses, which, as it was mentioned above, is an essential source contributing to the collision-induced FS. Thus, the three-segment scheme (Fig. 2) has a potential to further strengthen the optimization.

Results summarizing the dependence on the parameters d and D_3 (which corresponds to case 4 in Table 1) are collected in Fig. 5. Varying D_3 affects the average dispersion, therefore, in order not to alter its definition, the GVD parameters were subject to the constraint (cf. Equation (3))

$$L_1 D_1 + L_2 D_2 + D_3 d = 0, \tag{7}$$

so that the coefficients $\overline{D}_{u,v}$ correctly represent the average GVD.

To comply with the condition (7), it was necessary to choose parameters from the set of L_1, L_2, D_1, D_2, that are to be adjusted. To this end, two different natural options can be considered. The first is adjusting L_1 or L_2 so that $L_1 = -(L_2 D_2 + D_3 d)/D_1$ or $L_2 = -(L_1 D_1 + D_3 d)/D_2$. The second option is adjusting D_1 or D_2 so that $D_1 = -(L_2 D_2 + D_3 d)/L_1$ or $D_2 = -(L_1 D_1 + D_3 d)/L_2$. In fact, we started with values similar to those used in the simulations of the two-step model (see above): $L_1 = 2/5$, $D_1 = 5/2$, $L_2 = 3/5$, $D_2 = -5/3$ and, after choosing D_3 and d, the lengths were adjusted, rather than the GVD coefficients, as it was concluded that, following this option, much larger regions could be found in which the FS and TS are small. In addition, changing the lengths, rather than the GVD coefficients, is, obviously, a more realistic approach to tuning parameters of a real fiber-optic link. In Fig. 5(a) and (b), one sees that, indeed, both the FS (Fig. 5(a)) and TS (Fig. 5(b)) may be made smaller by means of choosing D_3 different from D_2.

To achieve the optimal operation regime, it is best to select parameters that make FS and TS small *simultaneously*. Indeed, the minimization of the FS is most appropriate for a long link containing many DM periods, while for relatively short links, consisting of several cells, most relevant is direct minimization of the TS. Thus, simultaneous minimization of both shifts will guarantee *homogeneous optimization* of a heterogeneous fiber-optic network, which is the objective of major practical interest.

Taking, for instance, the data corresponding to Fig. 5(a) and (b), we were indeed able to identify parameter regions where the simultaneous minimization of FS and TS is possible; the resulting double-optimum areas are shown in Fig. 6 (the shaded area). As an example produced by this double-optimization procedure, one can take parameter values close to $d = 0.15$ and $D_3 = -5$. The optimum regions resulting from this procedure slightly change with the variation of the total propagation length.

5.2. COMPARING THE NUMERICAL AND SEMI-ANALYTIC RESULTS

The semi-analytical prediction for the FS given by Equation (5e) was compared with the results of direct simulations. A typical example of the comparison is displayed in Fig. 7, which shows the semi-analytical results for the same case that was used to obtain the numerical results shown in Fig. 5(a). This and other examples demonstrate a qualitative, although not extremely accurate, agreement. The difference between the semi-analytical and numerical results is relatively sensitive to the value of the initial chirp Δ_0.

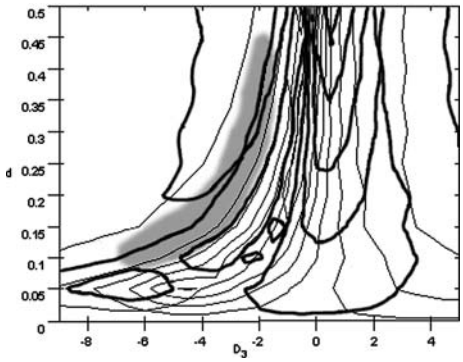

Fig. 6. Juxtaposition of contour plots of the FS (thin curves) and TS (thick curves), which correspond, respectively, to Fig. 5(a) and (b), produces the shaded region where *both* shifts take small values *simultaneously*.

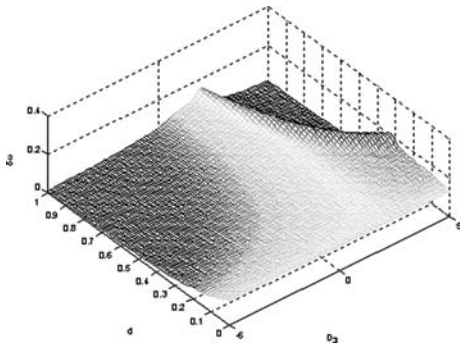

Fig. 7. The FS for the same case as in Fig. 5(a), but as found using the semi-analytical result (5e).

Such differences may be expected, since SPM (nonlinear intra-channel) effects are not included in the semi-analytical results.

5.3. SEARCH FOR A GLOBAL OPTIMUM

The above analysis focused on the optimization procedure based on the variation of parameters in pairs, while the other parameters were held fixed. We also searched for a *global* optimum by varying all the parameters that may be reasonably subject to variation, in order to find a global minimum of the FS in the *five-dimensional* parametric space $(d, D_3, \Delta_0, \overline{D}_{u,v}, \tau_0)$. In doing so, the variation of the parameters was confined to intervals $0.6 < \tau_0 < 1$, $1.5 < D_{u,v} < 1.5$, $-8 < D_3 < 5$, $0 < d < 0.3$, and $-5 < \Delta_0 < 5$. These intervals were suggested by the previous results obtained by varying the parameters in pairs. A global FS minimum was thus found at $\tau_0 = 0.8$, $D_{u,v} = -1.5$,

$D_3 = -4$, $d = 0.15$; the minimum is hardly sensitive to the value of Δ_0 if it is taken from the interval $5 < \Delta_0 < 5$. This finding is in agreement with the other results reported above. It is quite remarkable that the global optimum is achieved at a finite value of d and $D_3 \neq D_2$, i.e., the three-step model helps to improve the results indeed.

6. Summary and conclusions

We have systematically considered XPM-induced FS and TS of Gaussian pulses due to collisions in the two-channel prototype of a WDM system. The shifts were calculated semi-analytically, using a perturbative formula that generalizes the treatment of Kaup *et al.* 1999, and numerically by dint of direct simulations of the coupled nonlinear Schrödinger equations. The consideration was focused on the most dangerous case, when the two pulses completely overlap in the initial configuration. In addition to the straightforward two-segment model, a more sophisticated three-segment one was proposed and analyzed.

The numerical and semi-analytical results were found to be in reasonable agreement, both showing that efficient minimization of the collision-induced shifts may be achieved by proper selection of the system parameters. We found that it is especially beneficial to add a third segment and tune its length and dispersion coefficient; in particular, the global minimum of the FS was found for this configuration. In addition to the separate minimization of the FS and TS, we have also investigated *simultaneous* minimization of both shifts in finite regions of the parameter space. The latter result suggests a possibility for uniform optimization of the operating regimes in heterogeneous networks, which incorporate shorter and longer links. An interesting finding is that the FS does not necessarily decrease monotonically with increase of the inverse-group-velocity difference between the channels.

Acknowledgements

We gratefully acknowledge useful discussions with R. Driben, M. Gutin, and A. Shipulin.

References

Ablowitz, M.J., G. Biondini, A. Biswas, *et al. Opt. Lett.* **27** 318, 2002.
Ablowitz, M.J., G. Biondini and E.S. Olson. *J. Opt. Soc. Am. B* **18** 577, 2001.
Ablowitz, M.J., T. Hirooka and G. Biondini. *Opt. Lett.* **26** 459, 2001.
Berntson, A., N.J. Doran, W. Forysiak and J.H.B. Nijhof. *Opt. Lett.* **23** 900, 1998.

Etrich, C., N.C. Panoiu, D. Mihalache, *et al. Phys. Rev. E* **63** 016609, 2001.
Haus, H. and Y. Chen. *Opt. Lett.* **24** 217, 1999.
Hirooka, T. and A. Hasegawa. *Opt. Lett.* **23** 768, 1998.
Iannone, E., F. Matera, A. Mecozzi and M. Settembre. *Nonlinear Optical Communication Networks*, Wiley-Interscience, New York, 1998.
Kaup, D.K., B.A. Malomed and J. Yang. *Opt. Lett.* **23** 1600, 1998.
Kaup, D.J., B.A. Malomed and J. Yang. *J. Opt. Soc. Am. B* **16** 1628, 1999.
Kurtzke, C. *IEEE Photon. Technol. Lett.* **5** 1250, 1993.
Liu, X., X. Wei, L.F. Mollenauer, C.J. McKinstrie and C. Xie. *Opt. Lett.* **28** 1412, 2003.
Malomed, B.A. *Prog. Opt.* **43** 71, 2002.
McKinstrie, C.J. *Opt. Commun.* **205** 123, 2002.
Mollenauer, L.F., S.G. Evangelides and J.P. Gordon. *J. Lightwave Technol.* **9** 362, 1991.
Niculae, A.M., W. Forysiak, A.J. Gloag, J.H.B. Nijhof and N.J. Doran. *Opt. Lett.* **23** 1354, 1998.
Robinson, N., G. Davis, J. Fee, G. Grasso, P. Franco, A. Zuccala, A. Cavaciuti, M. Macchi, A. Schiffini, L. Bonato and R. Corsini. In: *Optical Fiber Communication Conference* (*OFC*), 1998 OSA Technical Digest Series, Vol. 2. Optical Society of America, Washington, DC, 1998, paper PD19.
Sugahara, H. *IEEE Photon. Technol. Lett.* **13** 963, 2001.
Sugahara, H., T. Inoue, A. Maruta and Y. Kodama. *Electron. Lett.* **34** 902, 1999.
Sugahara, H., H. Kato and Y. Kodama. *Electron. Lett.* **33** 1065, 1997; Devaney, J.F.L., W. Forysiak, A.M. Niculae and N.J. Doran. *Opt. Lett.* **22** 1695, 1997.
Sugahara, H. and A. Maruta. *J. Opt. Soc. Am. B* **18** 419, 2001.